Biology Direct

RESEARCH

Open Access

BRCA1 is involved in sustaining rapid antler growth possibly via balancing of the p53/endoplasmic reticulum stress signaling pathway

Qianqian Guo[1], Zhen Wang[1], Jiping Li[1], Chao Ma[1], Junjun Zheng[2], Hengxing Ba[1], Guokun Zhang[1*] and Chunyi Li[1*]

Abstract

Background Regeneration is the preferred approach to restore the structure and function after tissue damage. Rapid proliferation of cells over the site of damage is integral to the process of regeneration. However, even subtle mutations in proliferating cells may cause detrimental effects by eliciting abnormal differentiation. Interestingly deer antlers, arguably the fastest regenerating mammalian tissue, have not been reported, thus far, to grow malignant tumors. They provide a mammalian model to understand the possible mechanism by which rapid regeneration is achieved while avoiding the development of malignancies. Antler regeneration is based on the proliferation and differentiation of antler stem cells (AnSCs).

Results We identified 39 hub genes which may function in regulating the balance between rapid proliferation and genomic stability in the AnSCs during antler regeneration. Among these 39 genes, the tumor suppressor gene, BRCA1, was found to be more sensitive to DNA damage in the AnSCs compared to that in the deer somatic cells, and BRCA1 deletion in the AnSCs via CRISPR/Cas9 resulted in significantly higher levels of DNA damage. Lack of BRCA1 promoted cell apoptosis and cell senescence and inhibited cell proliferation and cell self-renewal. RNA-seq results showed that in the absence of BRCA1, the p53 signaling pathway was significantly up-regulated. Associated with this change, the cell apoptosis and cell senescence-relevant-genes, CDKN1A, CDKN2A and Fas were over expressed, but the expression of cell-cycle-progression-related genes was inhibited. In addition, BRCA1 expression levels were found to be more sensitive to endoplasmic reticulum stress (ERS) in the AnSCs compared to the somatic cells. Deletion of BRCA1 gene aggravated ERS and ERS-induced cell apoptosis.

Conclusions Our results revealed that BRCA1 is involved in sustaining rapid antler growth possibly via promotion of DNA damage repair that acts to maintain genome stability while protecting cells from p53/ERS-induced cell death. Understanding the mechanisms underlying the role played by BRCA1 in the process of antler regeneration is of great significance not only for regenerative medicine, but also for the understanding of cancer development.

Keywords Antler regeneration, BRCA1, Genome stability, p53

*Correspondence:
Guokun Zhang
zhang-guokun@hotmail.com
Chunyi Li
lichunyi1959@163.com
Full list of author information is available at the end of the article

Introduction

The precise regulation of DNA replication is vital for cellular division and genomic integrity [1], especially in rapidly proliferating cells, which are more susceptible to mutations during DNA replication, where even subtle mutations may cause genomic instability and aberrant differentiation or malignant transformation [2]. It is well known that regeneration after tissue or organ damage involves rapid cell proliferation [2]. Regeneration enables restoration of structural and functional integrity of the damaged tissue/organ [3]. However, there is experimental evidence indicates that regeneration and tumorigenesis are correlated, whereby a dysregulated process of regeneration may lead to neoplasia [3–5]. In invertebrates, in lower vertebrates and in mammals, the essence of regeneration is the proliferation of various types of cells on the damaged plane/stump to build up the lost parts [3]. However, mutation is a risk and the avoidance of any detrimental consequences of an increase in the rate of mutation during rapid cell proliferation while at the same time achieving rapid regeneration is an issue that must be resolved in regenerative medicine. To this end, appropriate animal models, particularly mammalian models, that are capable of rapid full regeneration without becoming cancerous are required. Recent advances in revealing the molecular mechanisms of antler regeneration [6, 7] have highlighted the potential of this mammalian model of natural regeneration whereby even with extreme rates of cell proliferation, the resultant-tissue remains remarkably cancer-free [8, 9].

Deer antlers are the only mammalian appendages that are once lost, can fully regenerate from the pedicles [10, 11]. The rate of growth of the regenerating antler can reach 2 cm per day, making them arguably the fastest growing mammalian tissue [10]. Antler regeneration relies on the periosteum of the pedicle (PP), a bony protuberance permanently covered by skin from which antlers are cast and regenerate annually [9, 12, 13]. Each year, around 3.3 million PP cells participate in each round of antler regeneration and give rise up to 15 kg of antler tissue mass in less than 3 months [11, 14, 15]. Activated PP cells are in a state of rapid cell division, which is comparable to or even faster than that in cancer cells, but in contrast to tumors, the process is tightly regulated [10]. This suggests that revealing the mechanism as to how such rapidly proliferating mammalian cells balance rapid proliferation and genomic stability is of great significance not only for regenerative medicine, but also for the understanding of cancer development.

Given PP cells have stem cell attributes they have been termed antler stem cells (AnSCs) [16, 17]. The initiation of antler regeneration is a process whereby the potentiated PP (PoPP) progresses to an activated PP (AcPP, also known as blastema) [13]. Although potentiated AnSCs (PoAnSCs, resident in PoPP) have acquired the ability to regenerate antler, only the activated AnSCs (AcAnSCs, resident in AcPP) rapidly proliferate to form a regenerating antler [6, 13, 17]. In our previous studies, we have found that there were significant differences in gene expression profiles between the AcAnSCs and PoAnSCs [13]. Therefore, the objective of the present study was to identify the key differentially expressed genes (DEGs), which might function in regulating the balance between rapid AcAnSC proliferation and the maintenance of their genome stability.

Here, we identified 39 such hub genes, among which a tumor suppressor gene, breast cancer type 1 susceptibility protein (BRCA1), was highly differentially expressed in the AcAnSCs compared to the PoAnSCs. We found that BRCA1 in the AnSCs was more sensitive to DNA damage compared to the other types of deer somatic cells. Functional analysis showed that BRCA1 positively regulated the response to the DNA damage for the maintenance of genome stability and negatively regulated the response to the endoplasmic reticulum (ER) stress and the p53/TGF-β signaling pathways for the enhancement of cell survival. In conclusion, our results suggest that BRCA1 may be a key regulator in sustaining the extremely rapid cell proliferation and at the same time maintaining the genome stability during antler regeneration. Understanding the underlying mechanism could give insight into a mammalian system where rapid epimorphic regeneration is initiated whilst genome stability is effectively mai ntained.

Materials and methods

Cell culture

The AcPP and PoPP were obtained in a previous study [13]. Procedures for culturing the AcPP and PoPP cells, i.e., AcAnSCs and PoAnSC, were conducted as described previously [13]. The cell culture system was: Dulbecco's Modified Eagle Medium (Life, USA) supplemented with 100 U/ml penicillin, 100 μg/ml streptomycin (Invitrogen, USA) and 10% fetal bovine serum (HyClone, Beijing, China), in a humidified incubator with 5% (v/v) CO_2 atmosphere at 37 °C. Cells used in this study had reached the third passage.

Plasmid construction

The sgRNAs targeting the deer BRCA1 gene were designed using the CRISPR Design tool (http://www.rgenome.net/cas-offinder/). The sgRNA oligonucleotides were annealed, cloned into the sgRNA expression vectors (Px458 plasmid, a gift by Dr. Yuan from Jilin University), then gel purified using a Gel Extraction Kit (Qiagen, Germany). The resultant constructs were subjected to Sanger

sequencing to verify proper sub-cloning of the sgRNA sequences. The detailed sgRNA sequences are provided in Table 1.

Electroporation and selection of BRCA1$^{-/-}$ cell clones

For electroporation, AcAnSCs (5×10^4 cells) at the third passage were mixed with recombinant plasmid (2.5 μg) in the electroporation buffer as described previously [18]. The mixture was loaded into the Neon Tip and electroporated at 1350 V using 30-ms pulse 1 time using the Neon Transfection System, according to the manufacturer's protocol (Thermo Fisher Scientific). The cells were plated into 10 cm cell plates at an appropriate density and incubated for one week; the cell clones were then picked and cultured in 24-well plates. Approximately one-quarter of each cell clone was digested and lysed with 10 μL of NP40 lysis buffer. The primer sequences for genotyping are as follows: Forward: AGGCTTTGGTCATTAGTT CTATGGT; Reverse: CCTTACCATCTTAAGGTCAAT TCAA.

Cell proliferation

Cell proliferation was measured using the Cell Counting Kit-8 (Solarbio, Beijing, China) and 5-Ethynyl-20-deoxyuridine (EDU) incorporation assay according to the manufacturer's instructions. Briefly, for CCK-8 assay, cells were seeded in 96-well plates at the density of 5×10^3 cells/well and cultured with 200 μL DMEM in 5% CO_2 at 37 °C for 3 days, then 20 μL CCK-8 solution (Beyotime, Nanjing, China) was added to each well, and the cells were cultured for 1 h. Absorbance was measured at 450 nm with a microplate analyzer. For the EDU incorporation assay, cells were incubated in the medium supplemented with 50 μM EDU for 3 h, fixed in 4% PFA for 30 min, then permeabilized in 0.5% Triton X-100 for 10 min and subsequently blocked with 3% bovine serum albumin (BSA) in PBS for 2 h. The nuclei of cells were counterstained with DAPI for 5 min in the dark. The specific fluorescent staining was examined under a fluorescent microscope (EVOS M5000, Thermo Fisher, USA).

Table 1 sgRNA sequences

Primer name	sgRNA sequence (5′ to 3′)
sgRNA1-F	CACCGaaagtatgggctaccggaac
sgRNA1-R	AAACgttccggtagcccatactttC
sgRNA2-F	CACCGtttatctgtggatcatgttg
sgRNA2-R	AAACcaacatgatccacagataaaC
sgRNA3-F	CACCGattctagccaaatgccagtc
sgRNA3-R	AAACgactggcatttggctagaatC

Cell apoptosis

Cell apoptosis was detected using an Annexin V-FITC Apoptosis Detection Kit (Beyotime, Nanjing, China) according to the manufacturer's instructions. Briefly, 1×10^6 cells were trypsinized using EDTA-free trypsin (Beyotime, Nanjing, China) and centrifuged at 1000 rpm, washed twice with PBS, then labeled with Annexin V-FITC and PI in binding buffer. Finally, the apoptotic populations of cells were detected with flow cytometry (BD Biosciences, USA).

Immunofluorescence staining

Cells were incubated in a 48-well plate and fixed with 4% PFA for 15 min, then permeabilized in 0.3% Triton X-100 for 10 min, and blocked by 3% BSA for 1 h at room temperature. Primary antibodies (rabbit anti-BRCA1, 1:200, Absin, abs134153; rabbit anti-γH2AX, 1:200, Abcam, ab11174) were added and incubated at 4℃overnight. After being washed with PBS, cells were incubated with fluorescent-labelled secondary antibodies (Invitrogen, USA) at room temperature for 1 h. The cell nuclei were counterstained with DAPI for 5 min in the dark. The images were captured under a fluorescence microscope camera (EVOS M5000, Thermo Fisher, USA).

Cell senescence

Cell senescence was assessed using a Cell Senescence β-galactosidase Staining Kit (Beyotime, china) according to the manufacturer's instructions. In brief, cells were seeded in 24-well plates at a density of 3×10^4 cells/well, and incubated at 37 °C, 5% CO_2 for 24 h, prior to staining. After fixation with 4% PFA, cells were stained with β-galactosidase staining solution and observed under a microscope (EVOS M5000, Thermo Fisher, USA); positive cells showed deep blue staining.

Protein preparing and Western blotting

Total cellular proteins were extracted and protein concentration measured using the BCA protein assay (Beyotime, China). Then, 30 μg protein was separated on a 10% sodium dodecyl sulfate polyacrylamide gel electrophoresis (SDS-PAGE) and transferred to 0.2-μm PVDF membranes. The membranes were subsequently blocked for 2 h in TBST containing 5% nonfat dry milk at room temperature, then incubated with specific antibodies (rabbit anti-BRCA1, 1:500, Absin, abs134153; rabbit anti-γH2AX, 1:500, Abcam, ab11174; rabbit anti-GRP78, 1:500, Absin) overnight at 4 °C. The blots were probed with HRP-conjugated secondary antibodies and detected using ECL and photographed.

Quantitative real-time PCR

Total RNA was isolated using TRizol reagent, purified on a silica base spin column (Qiagen, Germany), and then reverse-transcribed onto cDNA using the cDNA Synthesis Kit (Takara, Japan). The qRT-PCR assay was performed using the SYBR Kit (TransGen Biotech, Beijing, China) according to the manufacturer's protocol. Glyceraldehyde-3-phosphate dehydrogenase (GAPDH) was used as an endogenous control. Relative expression was calculated using the $2-^{\Delta\Delta CT}$ method to assess the fold change in expression levels of the target genes. Primer sequences are in Table S1.

RNA-seq

The RNA-sequencing (RNA-seq) data of AcPP and PoPP tissues are from previous studies [13]. The comparative RNA-seq of AcAnSC between BRCA1-/- and Control groups was performed by the Novegene Company (Beijing, China). The total RNA of cells was extracted using TRIzol reagent (Qiagen, Germany) according to the manufacturer's procedure. RNA quality was confirmed using a bioanalyzer with a minimum RNA integrity number of 7. Sequencing libraries were generated using NEBNext Ultra RNA Library Prep Kit for Illumina (NEB, USA, Catalog #: E7530L) following manufacturer's recommendations.The qualified libraries were pooled and sequenced on Illumina platforms with PE150 strategy in Novogene Bioinformatics Technology Co., Ltd (Beijing, China), according to effective library concentration and data amount required. High quality reads were aligned to the Cervus nippon (Sika deer) reference genome MHL_v1.0 [19] by HISAT (v2.0.4). The transcript quantification (FPKM, fragments per kilobase per million) was calculated using RSEM. Genes meeting the criteria set at |Fold Change)|> 1.5, and the false discovery rate (FDR) < 0.05 were assigned as differentially expressed.

Hub gene identification

The hub genes, which interact most frequently with other genes and act like a hub in a network, were selected by Cytohubba (version: 0.1) [20] and CytoNCA plugin (version:2.1.6) [21]. Each of the two applications were respectively used to screen out the top 100 nodes in four methods (CytoNCA: Betweenness, Closeness, Degree and Eigenvector; CytoHubba: EPC, MCC, MNC, and Stress). Linear correlations between hub genes were assessed using the Pearson correlation coefficient (R software, version 3.6, https://www.R-project.org/.).

Statistical analysis

The results are presented as mean ± SEM. Statistical significance was evaluated using GraphPad Prism 9.0.0 (GraphPad Software, La Jolla, CA, United States) software. Statistical analysis for the comparisons of multiple variables was performed using a two-way ANOVA, and Student's t-test was used to compare two variables. All experiments were performed in triplicate at least. The values were set at $p < 0.05$ for statistical significance.

Results

BRCA1 identified as a highly expressed hub gene in the activated antler stem cells (AcAnSCs)

In our previous study, we performed RNA-seq analysis between the PoPP and AcPP (Fig. 1A) and identified a group of differentially expressed genes (DEGs) [13]. In the present study, we sought to identify regulators that might be candidates for sustaining the rapid proliferation of the AcAnSCs while maintaining genomic stability. Therefore, we re-analyzed the sequencing data and generated information about the interactions among the up-regulated DEGs and the PPI network using the STRING online database. In total, 932 up-regulated DEGs were filtered into the PPI network with 613 nodes and 6491 edges, at a combined score ≧ 0.4 and were grouped using the Cytoscape software. Four clusters were screened with a cut-off k-score = 5 depending on the MCODE scoring system (Fig. 1B; Supplementary Table 2). To identify key biological processes in which up-regulated DGEs were involved, GO enrichment analysis was performed using the MetAnSCape system (Supplementary Tables 3–6). In Cluster 1, the up-regulated DEGs with the highest score were found to be mainly related to regulation of cell proliferation, such as cell division, cell cycle phase transition, and positive regulation of the cell cycle process. Hub genes in the up-regulated DEGs in the AcAnSC were detected using the CytoHubba and CytoNCA software (Fig. 1C). Finally, 39 hub genes (e.g. CDK1, CCNB1, BRCA1) were identified. We then calculated Pearson correlation coefficients between these 39 hub genes and found a significant correlation amongst them (Fig. 1D). Pathway analysis showed that the main biological process and pathways in which these node genes were involved fell in the category of regulation of cell cycle, DNA replication, the p53 signaling pathway, and the regulation of DNA repair (Fig. 1E; Supplementary Table 7). The first two pathways are related to cell proliferation and the other two are related to genomic stability, supporting the proposition that the AcAnSCs possess a rigorous mechanism for balancing rapid proliferation and genomic stability. Amongst these hub regulators, we identified an important tumor suppressor gene, BRCA1, that was highly expressed in the AcAnSCs.

To further investigate the findings relating to BRCA1 expression level from the RNA-seq analysis, we carried out immunofluorescent staining of the AcPP and PoPP tissues. The results showed that BRCA1-positive cells

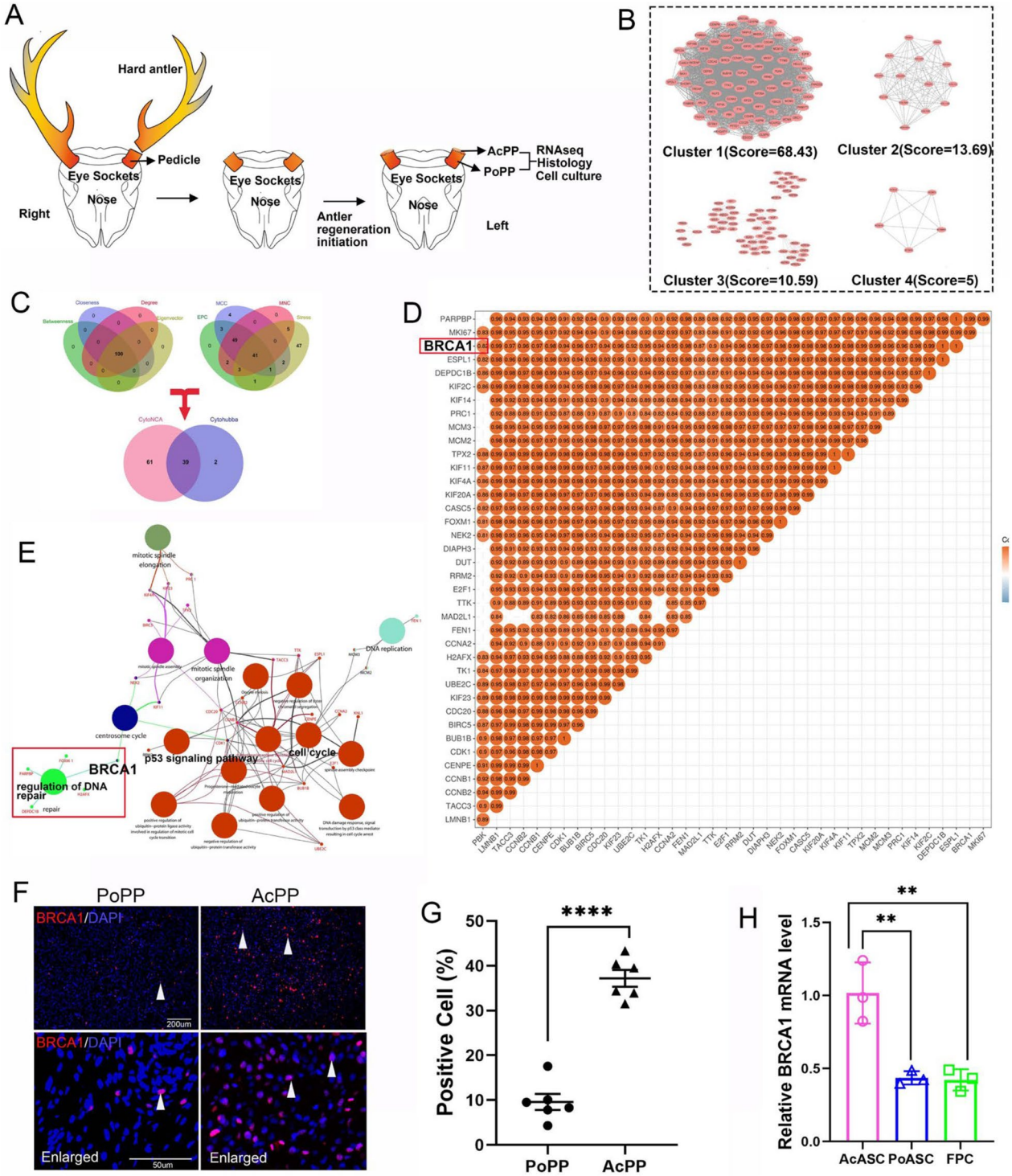

Fig. 1 BRCA1 is identified as a highly expressed hub gene in the AcASCs. **A** Initiation of antler regeneration is a process from PoPP to AcPP. **B** Module analysis of all up-regulated DEGs between the AcPP and PoPP. **C** Venn diagram showing 39 overlapping (hub) genes applying two different calculation methods (CytoNCA and Cytohubba) for the up-regulated DEGs. **D** Correlation Heatmap of the 39 hub genes (P value < 0.05). **E** Enrichment results of GO biological process and KEGG pathways constructed using 39 hub genes via ClueGO and CluePedia plugins. **F** Immunofluorescent staining of BRCA1 (white arrows) in the AcPP and PoPP tissues. **G** Percentage of BRCA1 positive cells. Data are shown as the mean ± SEM, n = 6, $^{**}p < 0.01$; $^{****}p < 0.0001$. **H** Relative expression levels of BRCA1 mRNA in the AcAnSCs, the PoAnSCs and FPCs. Data are shown as the mean ± SEM, n = 3, $^{**}p < 0.01$; $^{****}p < 0.0001$

were only sparsely scattered in the PoPP, but there was a dense population in the AcPP (Fig. 1F). Cell counting (Fig. 1G) showed that percentage of BRCA1-positive cells in the AcPP (37.2% ± 1.86%) was significantly higher ($p < 0.0001$) than that in the PoPP (9.60% ± 1.79%). Next, we analyzed the gene expression status of BRCA1 at the cellular level. As shown in Fig. 1H, BRCA1 mRNA level in the AcAnSCs was significantly higher than that in the PoAnSCs and the control somatic cells (facial periosteum cells, FPCs). Together these findings show that BRCA1 was highly expressed in the AcAnSCs and was confirmed as a hub gene, which suggests that BRCA1 may be an important factor that plays a role in balancing rapid proliferation and genome stability during antler regeneration.

BRCA1 deletion in AcAnSCs impaired cell proliferation and colony formation

To test the direct effects of BRCA1 on the AcAnSCs in vitro, we knocked out BRCA1 in the AcAnSCs via CRISPR/Cas9. Three sgRNAs targeting the BRCA1 gene were designed (Fig. 2A) with sequencing showing that BRCA1-sg1 was the most effective (Supplementary Fig. 1A-1B). Ten single-cell clones were picked and characterized, with two homozygous clones (clone 1# and clone 2#) identified as having genetic mutations (Fig. 2B). To confirm if deletion of BRCA1 was successful at the protein level, western blot analysis and immunofluorescent staining were performed (Fig. 2C, D). The results showed that clone 2# exhibited no band of BRCA1 protein, but clone 1# did (Fig. 2C). We therefore selected clone 2#, which was termed BRCA1-/- group. In the following descriptions, the WT clone was termed the Sham group, and the AcAnSC cells that were not subjected to electroporation process were termed the Control group.

To explore the effects of BRCA1 deletion on cell proliferation, CCK-8 and EDU incorporation assays were conducted. As shown in Fig. 2E, on the third day of cell culture, the cell proliferation rate of AcAnSCs in the BRCA1-/- group (0.91 ± 0.04) was significantly lower than that in the Control (2.18 ± 0.11) and in the Sham groups (1.65 ± 0.04). Likewise, significantly fewer dividing cells (EdU positive) were detected in the BRCA1-/- group (10.1 ± 1.75%) than in the Control (38.9 ± 1.72%) and Sham (29.2 ± 2.0%) groups (Fig. 2F and H). Furthermore, a colony formation assay was performed to test the ability for cell self-renewal. Single cells from the Control (59.7 ± 1.45) and Sham groups (50.7 ± 2.03) generated colonies on day 14, but there was no obvious colony formation in the BRCA1-/- group (1.0 ± 0.56; Fig. 2G and I). Taken together, these results provide robust evidence that BRCA1 deletion impaired proliferation and self-renewal of the AcAnSCs in vitro.

BRCA1 deletion in AcAnSCs promoted cell apoptosis and cell senescence

To explore the possible causes of the observed inhibitory effect on cell survival and self-renewal due to BRCA1 deletion, we examined the status of both cell apoptosis and cell senescence in the BRCA1-/- group. As shown in Fig. 3A, numerous apoptotic cells were observed in the BRCA1-/- group, while only a few were seen in the other two groups. Quantitative analysis showed that the numbers of both early-apoptotic and late-apoptotic cells in the BRCA1-/- group (5.2 ± 0.23%; 12.4 ± 0.66%) were significantly higher than those in the Control (1.8 ± 0.35%; 1.5 ± 0.12%) and Sham groups (2.1 ± 0.26%; 1.4 ± 0.03%) respectively (Fig. 3C).

To investigate the effects of knockout of BRCA1 gene on cell senescence, β-galactosidase staining was carried out. As shown in Fig. 3B, cells in the Control group were barely stained. In sharp contrast, the percentage of positively stained cells for β-galactosidase increased in both the BRCA1-/- and Sham groups, indicating that these cells were undergoing senescence (Fig. 3B). The cell size was increased in the BRCA1-/- group compared to the other two groups. Quantitative analysis (Fig. 3D) showed that percentage of aging cells following BRCA1 knockout (57.3 ± 2.91%) was significantly increased compared to the Control (9.6 ± 1.28%) and Sham groups (27.2 ± 2.07%). These results suggest that BRCA1 deletion in the AcAnSCs promotes cell apoptosis and cell senescence.

BRCA1 deletion in AcAnSCs promoted DNA damage and UV-induced apoptosis

Since BRCA1 contributes to DNA repair and transcriptional regulation in response to DNA damage [22], we investigated changes in its expression levels upon UV irradiation that is known to cause DNA damage. As shown in Fig. 4A, all cells exhibited a significant increase in BRCA1 mRNA level after irradiation. In the AcAnSCs, the expression level of BRCA1 was up-regulated nearly seven-fold, but only three-ford in the FPCs, indicating that changes in BRCA1 expression levels are more sensitive in response to DNA damage in the AcAnSCs than in the FPCs.

Next, we detected the effects of BRCA1 knockout on the response to DNA damage using γ-H2AX staining. As shown in Fig. 4B, cells in the Control and Sham groups showed virtually no signal for γ-H2AX; in contrast, a substantial level of γ-H2AX-positively staining was observed in the BRCA1-/- group, suggesting the DNA damage occurred. After UV irradiation, cells in all three groups formed large numbers of nuclear γ-H2AX foci, and the positive staining was stronger and the nuclear γ-H2AX foci were significantly higher in the BRCA1-/- group than in the other two groups (Fig. 4B, C). The quantitative

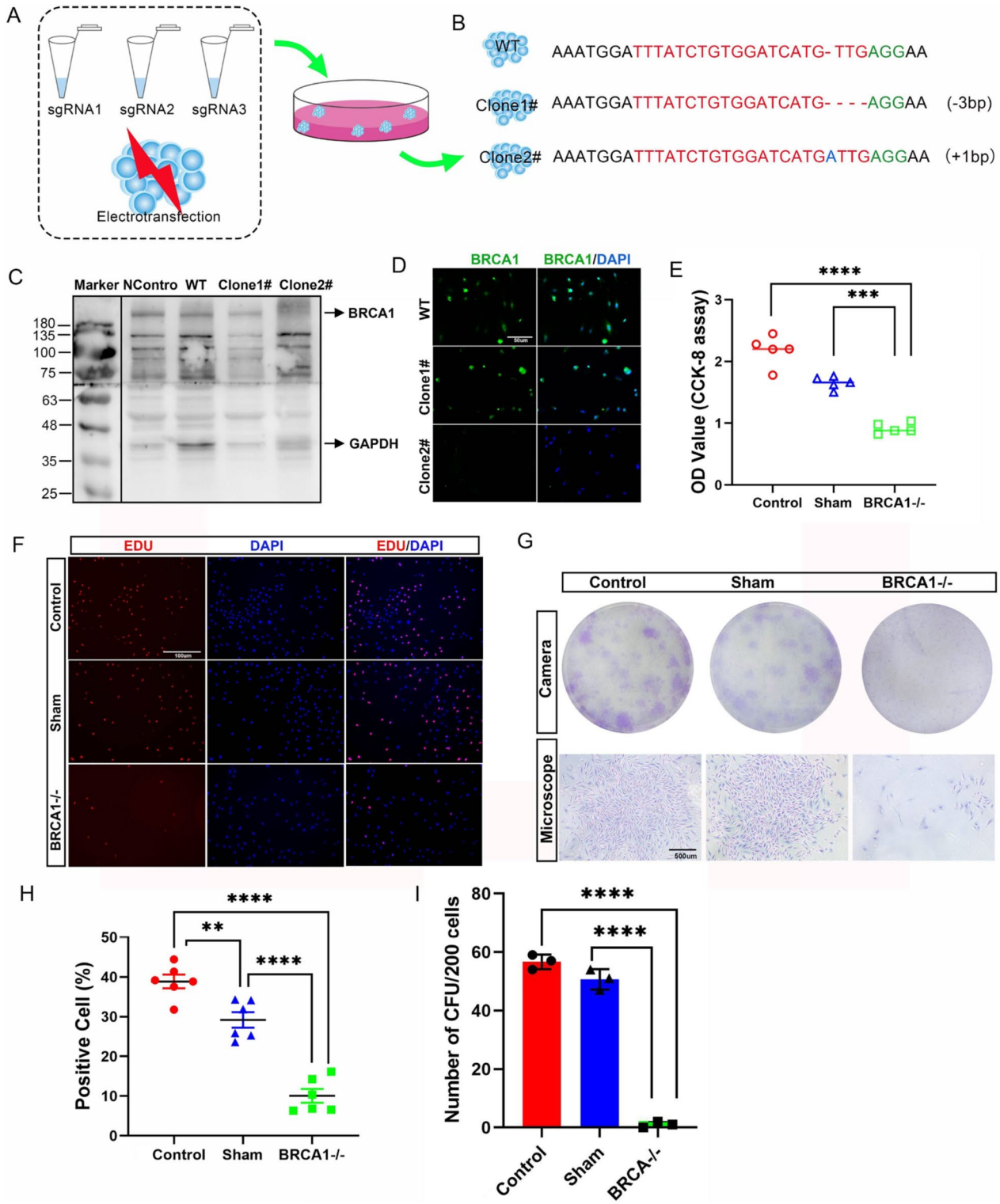

Fig. 2 BRCA1 deletion in the AcAnSCs impaired cell survival. **A** Flow chart of cell electroporation and cell clone selection. **B** Sequencing analysis of cell clones; note that two clones were identified as having genetic mutations. **C** Western blot analysis of BRCA1 protein expression; note that clone 2# exhibited no BRCA1 protein band but clone 1# did. **D** Immunofluorescent staining of BRCA1. **E** Cell proliferation evaluated via CCK-8 assay; data are shown as the mean ± SEM, n = 5, ***$p < 0.001$; ****$p < 0.0001$. **F** Proliferation cells (red fluorescence) in the different groups via EdU incorporation assay. **G** Colony-forming units (CFUs) (top) and a single CFU (bottom). **H** Percentage of EdU positive cells; data are shown as the mean ± SEM, n = 6, **$p < 0.01$; ****$p < 0.0001$. **I** Number of CFUs; data are shown as the mean ± SEM, n = 3, ****$p < 0.0001$

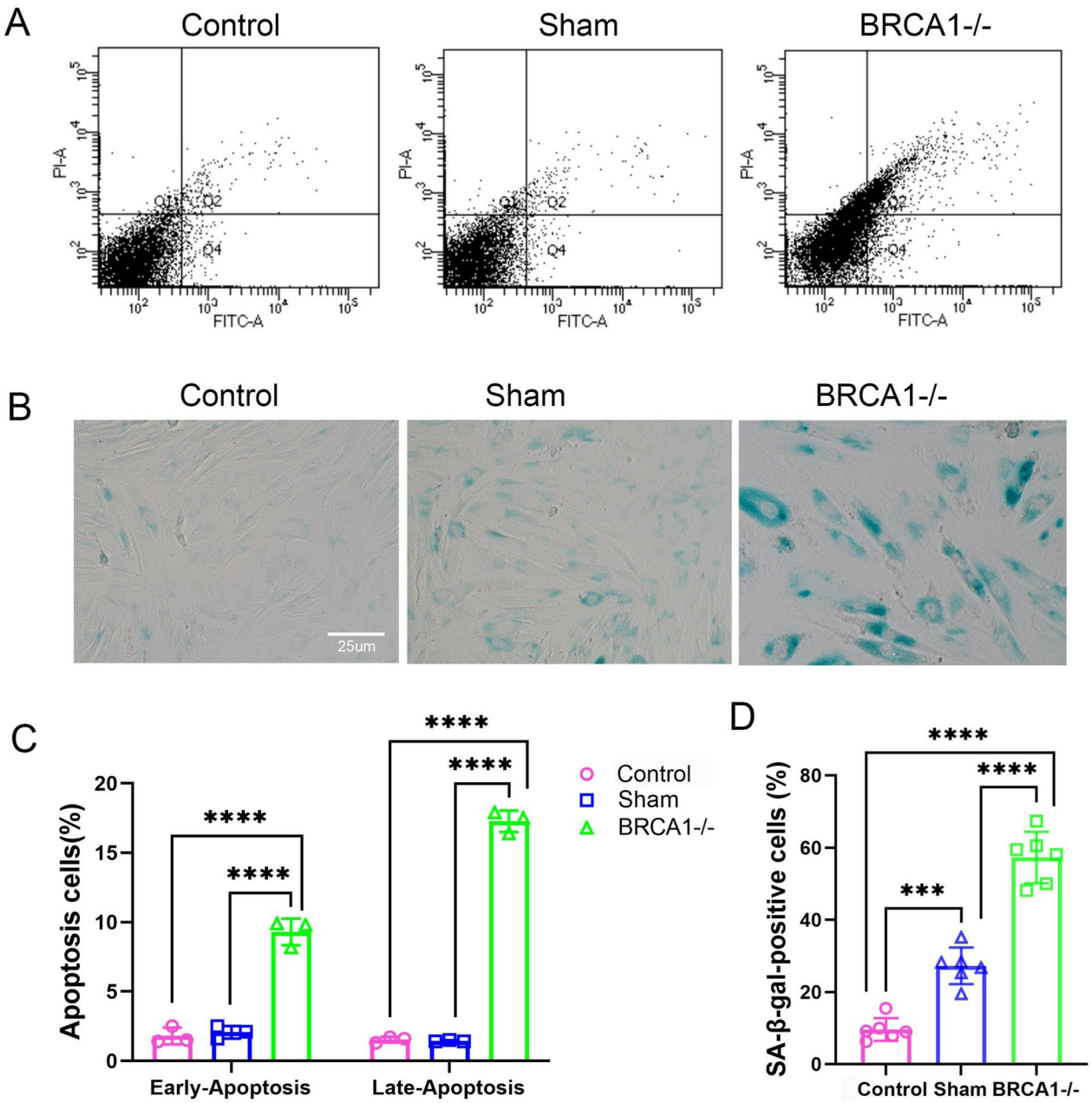

Fig. 3 BRCA1 deletion promoted apoptosis and senescence of the AcAnSCs. **A** Cell apoptosis analysis using flow cytometry. **B** Cell senescence analysis via β-galactosidase staining. **C** Percentage of early-apoptotic and late-apoptotic cells in the different groups; note that numbers of early-apoptotic and late-apoptotic cells in the BRCA1-/- group were significantly higher than those in the Control and Sham groups; data are shown as the mean ± SEM, n = 3, ****$p < 0.0001$. **D** Percentage of senescent cells in the different groups; the results showed that the percentage of aging cells following BRCA1 knockout was significantly increased compared to the Control and Sham groups. Data is shown as the mean ± SEM, n = 6, ***$p < 0.001$; ****$p < 0.0001$

analysis showed that the number of γ-H2AX foci per cell was higher in the BRCA1-/- group (4.9 ± 0.83) than in the Control (1.3 ± 0.26) and Sham groups (1.3 ± 0.57) (Fig. 4D); the percentage of γ-H2AX positive cells (foci > 50) was significantly higher in the BRCA1-/- group than in the Control and Sham groups (Fig. 4E). Consistent with the immunofluorescent staining results, western blot analysis showed that the expression level of γ-H2AX in the BRCA1-/- group was significantly higher than that in the Sham group (Fig. 4F, G). Further, our flow cytometry results showed that loss of BRCA1 resulted in significant increase in cell apoptosis upon UV irradiation.

Quantitative analysis showed that the number of apoptotic cells in the BRCA1-/- group were significantly higher than the other groups (Fig. 4H, I). These results show that BRCA1 deletion in the AcAnSCs impaired DNA damage response, which is known to be crucial for the maintenance of genomic stability, and also promoted UV-induced cell apoptosis.

BRCA1 deletion activated the p53/TGF-β signaling pathway

To identify the mechanism underlying the impairment of cell proliferation and genomic stability of the AcAnSCs after BRCA1 deletion, we conducted comparative RNA-seq analysis between the Control and BRCA1-/- groups. We performed signaling pathway analysis on the annotated genes that changed significantly upon BRCA1 deletion (Fig. 5A) and found that most of those DEGs were involved in the cancer pathway, the MAPK signaling pathway, the p53 signaling pathway and the TGF-β signaling pathway as well as the cellular senescence and the breast cancer pathway. Gene set enrichment analysis (GSEA) was then applied to identify the most prominent biological processes, and the results showed that the p53 signaling pathway (Fig. 5B), the TGF-β signaling pathway (Fig. 5C) and the protein processing in endoplasmic reticulum pathway (Fig. 5D), all of which are related to cell proliferation and genome stability or protein stability maintenance, were significantly up-regulated in the BRCA1-/- group. A heatmap for the differentially enriched genes in the p53 signaling pathway (Fig. 5E) showed that genes related to cell cycle progression (e.g. CCNB1, CCNB2) were mainly down-regulated, while the genes related to cell apoptosis and cell senescence (e.g. CDKN2A and FAS) were significantly up-regulated in the BRCA1-/- group, which may be a key contributor to the reduced cell proliferation rate. Gene expression level analysis for DEGs enriched in the TGF-β signaling pathway showed that genes of TGFB2 and TGFBR2 were significantly up-regulated, suggesting that in the AcAnSCs, BRCA1 may inhibit the TGF-β signaling pathway through suppression of transcription and secretion of TGFB2.

To further investigate the RNA-seq findings, we evaluated expression levels of some key genes involved in the p53 signaling pathway at the mRNA level. The results showed that the gene expression levels of CDK1, CDK2, CCNB1 and CCNB2 (Fig. 5F–I) were significantly lower, whereas CDKN1A, CDKN2A and Fas (Fig. 5J–L) gene expression levels were significantly higher in the BRCA1-/- group than in the Control and Sham groups. These results were consistent with the RNA-seq results. Therefore, our results show that BRCA1 deletion significantly impaired proliferation and self-renewal of the AcAnSCs, and caused death of these cells, likely at least partially through activation of the p53/TGF-β signaling pathway.

BRCA1 deletion induced excessive endoplasmic reticulum (ER) stress response

Recently, BRCA1 has been reported to mediate protein stability through regulation of the ER stress response [23]. In this study, BRCA1 deletion resulted in changes in gene expression profiles involved in the biological process of protein processing in the endoplasmic reticulum in the AcAnSCs. To investigate the relationship between BRCA1 and ER stress in the AcAnSCs, we examined changes in BRCA1 gene expression levels upon tunicamycin (TM) treatment, which is known to cause an ER stress response. As shown in Fig. 6A, expressions of BRCA1 mRNA in both the AcAnSCs and PoAnSCs were significantly increased after TM treatment, but there was no significant change in expression levels in the FPCs, indicating that BRCA1 expression levels in the AnSCs were more sensitive to ER stress than the somatic cells, such as FPCs.

To detect the effects of BRCA1 deletion on the ER stress response, we assessed the expression levels of GRP78, a representative marker of ER stress. AcAnSCs in the BRCA1-/- group showed increased levels in both protein and mRNA of GRP78 compared to those in the Control and Sham groups (Fig. 6B–D), indicating the increased ER stress in the AcAnSCs. Next, we examined the effect of BRCA1 deletion on TM-induced apoptosis. As shown in Fig. 6E, numerous apoptotic cells were observed in the BRCA1-/- group after TM treatment. Quantitative analysis showed that the percentage

(See figure on next page.)

Fig. 4 BRCA1 deletion in the AcAnSCs increased DNA damage and UV-induced apoptosis. **A** Relative expression levels of BRCA1 mRNA in the different groups after UV treatment; data are shown as the mean ± SEM, n = 3, ***$p < 0.001$; ****$p < 0.0001$. **B**, **C** Immunofluorescent staining of γ-H2AX. **D** The number of γ-H2AX foci per cell in the different groups; note that the number ofγ-H2AX foci per cell was higher in the BRCA1-/- group than in the Control and Sham groups; data are shown as the mean ± SEM, n = 5, **$p < 0.01$. **E** Percentage of γ-H2AX positive cells (foci > 50); note that the percentage of γ-H2AX positive cells was significantly higher in the BRCA1-/- group than in the Control and Sham groups; data are shown as the mean ± SEM, n = 5, *$p < 0.05$,***$p < 0.001$,****$p < 0.0001$. **F** Western blot analysis of γ-H2AX protein expression. **G** Relative expression levels of γ-H2AX protein; data are shown as the mean ± SEM, n = 3, *$p < 0.05$. **H** Cell apoptosis analysis using flow cytometry after UV-treatment. **I** Percentage of apoptotic cells in the different groups; data are shown as the mean ± SEM, n = 3, *$p < 0.05$, **$p < 0.01$

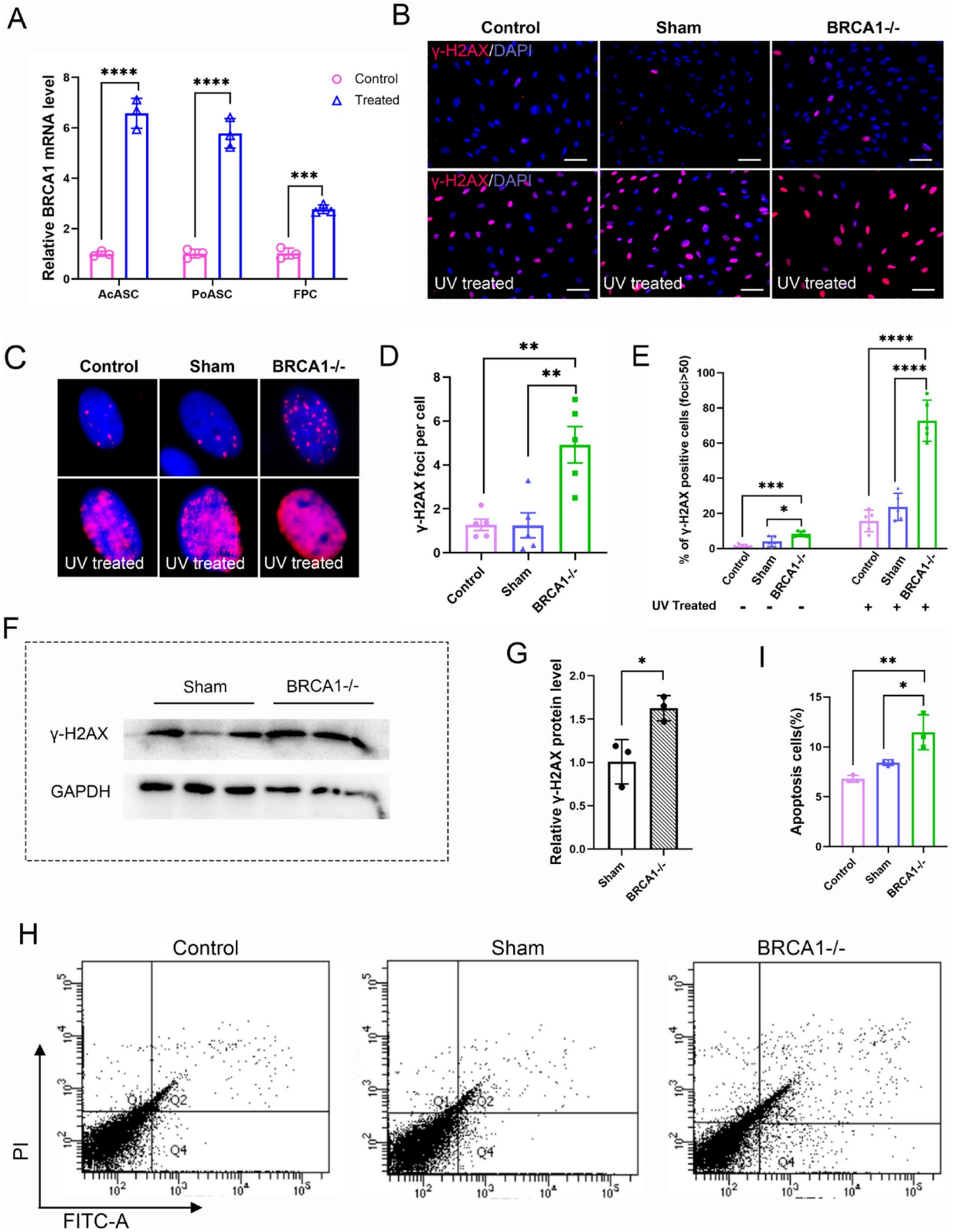

Fig. 4 (See legend on previous page.)

of apoptotic cells in all three groups increased after TM treatment, and the number of apoptotic cells in the BRCA1-/- group was significantly higher than those in the other two groups (Fig. 6F). In conclusion, increased cell apoptosis in the BRCA1-/- group may have been associated with an increase in ER stress, suggesting that in the rapidly proliferating AcAnSCs, BRCA1 may inhibit ER stress-induced cell death, and thus indirectly promote cell survival.

Discussion

This study focuses on the phenomenon of the very rapid, but cancer-free, growth of the antler during regeneration. Recent studies have found that the rapid regeneration of antler tissue involves adoption of oncogenic pathways without any evidence of growth being out of control as with tumor tissue [11]. This suggests that there must be potent regulators that precisely control rapid growth and confer protection against neoplastic transformation. By comparing the gene expression profiles of the PoAnSCs and AcAnSCs, we identified that BRCA1 was one of the highly significantly expressed genes in the AcAnSCs. BRCA1 is known as an important tumor suppressor [22] and in the present study was found to be more sensitive to DNA damage in the AnSCs than in the deer somatic cells, FPCs. Deletion of BRCA1 resulted in a significant increase in γ-H2AX foci, indicating enhanced DNA damage. Further functional analysis via gene knockout showed that deletion of BRCA1 inhibited proliferation and self-renewal of the AcAnSCs but promoted apoptosis and senescence of these cells. RNA-seq results showed that lack of BRCA1 protein significantly up-regulated p53 and TGF-β signaling pathways. In addition, our results demonstrated that changes in BRCA1 expression levels in the AnSCs were more sensitive than somatic cells in response to ER stress, and deletion of BRCA1 aggravated ER stress and ER stress-induced cell apoptosis in the AcAnSCs. Overall, our work suggests that BRCA1 is involved in sustaining extremely rapid antler growth via promoting effective DNA damage repair thereby maintaining genomic stability while protecting cells from p53/ERS-induced cell death (Fig. 7).

Antlers undergo extremely rapid growth, with the rate of cell proliferation surpassing even cancer cells [10, 11]. In this study, by comparing the gene expression profiles between the PoAnSCs and AcAnSCs, 39 hub DEGs were identified, most of which are related to cell cycle pathways, which is consistent with the phenomenon that cells are in a rapid proliferation mode. At the same time, we found that BRCA1 was highly expressed in the AcAnSCs and served as a prominent hub gene. BRCA1 is a well-known breast cancer tumor suppressor [24]. Mutations in BRCA1 gene lead not only to familial breast and ovarian cancers but are also the likely driver of a variety of sporadic cancers [25]. Mice deficient in BRCA1 have been shown to develop basal-like mammary carcinoma [26]. Therefore, we speculate that high expression of BRCA1 in the AcAnSCs may be associated with maintaining rapid proliferation while inhibiting cancer transformation.

BRCA1 has been implicated in a number of cellular processes, such as cell cycle control, cell proliferation, and transcriptional regulation [27]. Ontogenetic analysis of BRCA1 gene expression in the normal mouse showed that BRCA1 is highly expressed in rapidly proliferating cells [28]. It has been reported that cessation of BRCA1 expression in genetically-modified mice was associated with impaired cellular proliferation resulting in early embryonic lethality [29, 30]. Consistent with these reports, we found that loss of BRCA1 significantly inhibited proliferation and self-renewal of AcAnSCs, but promoted cell death, including enhanced cell apoptosis and senescence, indicating that BRCA1 can effectively promote cell survival ability, thus reinforcing the importance of BRCA1 in the rapidly proliferating AcAnSCs during antler regeneration.

It is known that rapidly proliferating cells are prone to DNA damage [25], and that BRCA1 plays a key role in DNA damage repair, especially via homologous recombination (HR) repair in response to DNA double-strand breaks (DSBs) [31, 32]. It has been reported that BRCA1 directly binds to DNA, thereby providing key evidence for the involvement of BRCA1 in DNA repair and replication fork maintenance [25, 33]. Recent studies have shown that BRCA1-deleted cells exhibit significantly impaired HR repair [34]. Here, we found that rapidly proliferating AnSCs were more sensitive to DNA damage than that in deer somatic cells FPCs, and deletion of BRCA1 resulted in an increased level of DNA damage, which may be attributed to the impaired BRCA1-related HR repair ability. These findings indicate that, in the

(See figure on next page.)

Fig. 5 BRCA1 deletion activated p53/TGF-β signaling pathway. **A** KEGG analysis of all DEGs between the Control and BRCA1-/- groups. **B**–**D** Gene set enrichment analysis (GSEA) of RNA-seq data; note that the p53 signaling pathway, the TGF-β signaling pathway and protein processing in the endoplasmic reticulum were activated. **E** Expression level of DEGs enriched in the p53 (left) and TGF-β (right) signaling pathways. **F**–**L** Evaluation of relative expression levels of CDK1, CDK2, CCNB1, CCNB2, CDKN2A, CDKN1A and Fas mRNA; data are shown as the mean ± SEM, n = 3, *$p < 0.05$, ****$p < 0.0001$

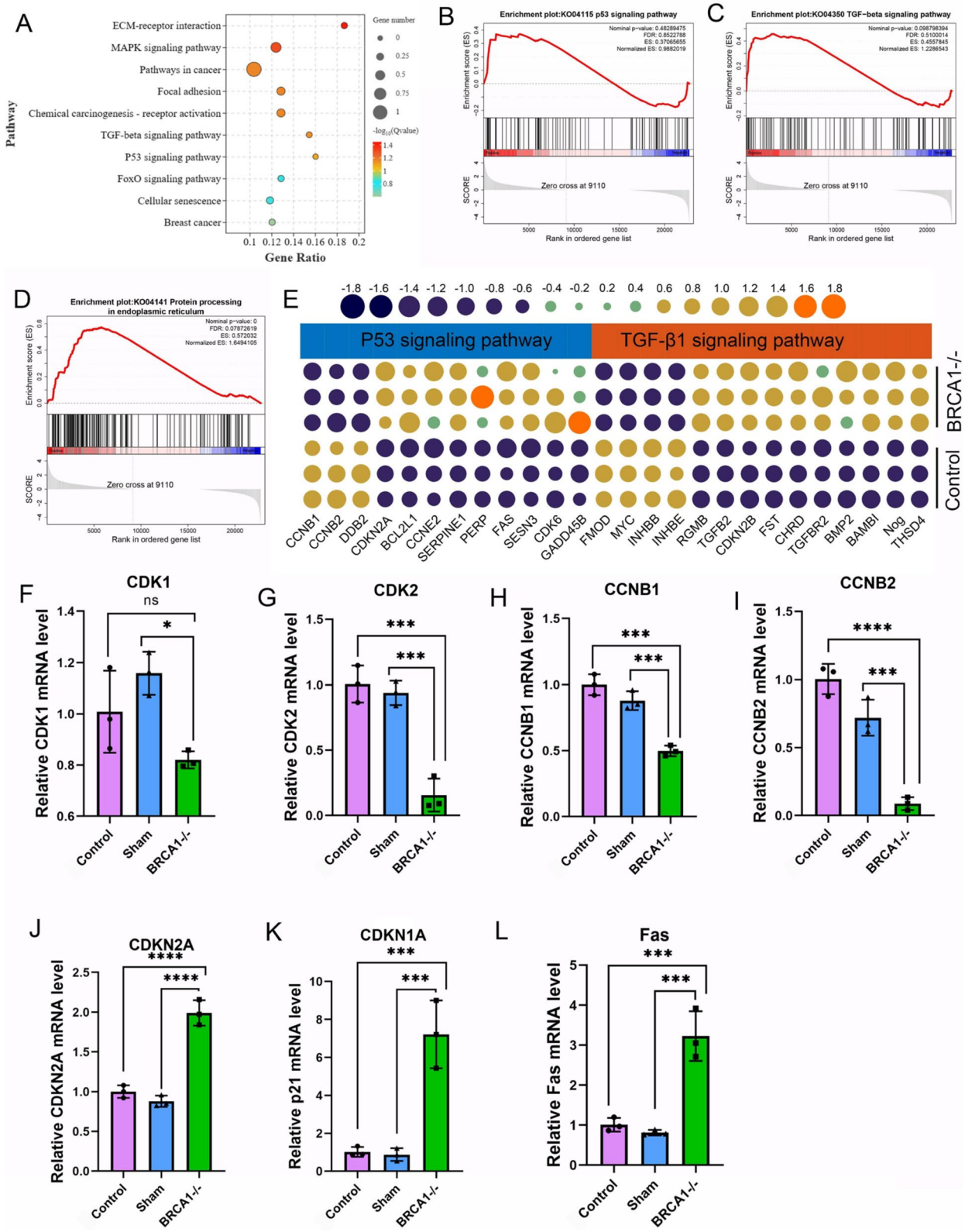

Fig. 5 (See legend on previous page.)

rapidly proliferating AcAnSCs, BRCA1 may contribute to the maintenance of genome stability by actively participating in HR repair.

In mammalian cells, in addition to HR repair, there are three other conserved, mechanistically distinct pathways for DSB repair, such as non-homologous end joining (NHEJ) [35]. NHEJ often entails deletion or insertion of several nucleotides and can also give rise to chromosome translocations. In contrast, HR is the most accurate DSB repair mechanism and is capable of faithfully restoring the original configuration of the broken DNA molecule [25]. HR and NHEJ operate as two distinctly different pathways and compete to process DNA break repair [36–38]. It has been reported that choice between DSB repair pathways is governed by the opposing activities of the p53 and BRCA1 proteins [36]. Loss of p53-binding protein 1 (53BP1) partially restores the HR defects caused by BRCA1 deficiency [34, 37]. In the present study, DEGs resulting from BRCA1 deletion were significantly enriched in the p53 signaling pathway; this included some that are involved in cell apoptosis and cell senescence including CDKN1A, CDKN2A and Fas. In contrast, DEGs involved in cell cycle progression were significantly inhibited, including CDK1 and CDK2. These results indicate that BRCA1 deletion may result in the p53-related NHEJ pathway being more favored. It is known that BRCA1 deletion leads to a severe proliferation defect [39], which is associated with extensive apoptosis and activation of the p53-related DNA damage response [40]. In the present study, we demonstrated that BRCA1 deletion led to impaired cell proliferation and increased cell apoptosis, suggesting that the underlying molecular mechanism may be associated with enhanced p53/DNA damage pathways. Overall, our results reveal that BRCA1, in helping to sustain rapid antler growth may be achieving this via balancing of the DNA damage/p53 signaling pathway.

In addition to the p53 signaling pathway, the TGF-β signaling pathway was also significantly up-regulated after knockdown of BRCA1 gene in the AcAnSCs. TGF-β signaling has been reported to suppress BRCA1-dependent DNA repair in response to DNA-damaging agents [41], and loss or reduction of BRCA1 was reported to alter the growth inhibiting activity of the TGF-β pathway [42]. In this study, our RNA-seq results further confirmed that most of DEGs were associated with the TGF-βsignaling pathway, indicating that BRCA1 deletion promotes the TGF-β signaling pathway, and the growth inhibiting activity of TGF-β pathway may be responsible for the impaired proliferation of BRCA1-/- AcAnSCs.

The BRCA1 protein was initially thought to be primarily located in the nucleus but recent studies have demonstrated that it is also found in other subcellular locations, including the endoplasmic reticulum (ER) [23, 43, 44]. It is reported that BRCA1 may be an important modulator of protein integrity through regulating the ER stress response [23]. In the present study, BRCA1 deletion resulted in the changes in gene expression profiles involved in the biological process of protein processing in the ER, and changes in BRCA1 expression levels in the AnSCs were more sensitive to ER stress than some somatic cells, such as FPCs. This finding suggests that effects of BRCA1 in the AcAnSCs may be exerted through involvement in the ER function. Rapidly proliferating cells are vulnerable to unfolded protein accumulation thus triggering an ER stress response; given this, we speculate that BRCA1 may be involved in regulating the ER stress response in the AcAnSCs. GRP78, a representative marker of the ER stress response, has been identified as a novel downstream target of BRCA1 [45]. In this respect, over-expression of wild-type BRCA1 suppressed the expression of GRP78, whereas expression of mutant BRCA1 gene or targeted inhibition of endogenous BRCA1 using small-interfering RNA (siRNA) enhanced GRP78 expression [45]. Consistent with these reports, our results showed that BRCA1 deletion increased expression levels of GRP78 protein and mRNA, suggesting the induction of an excessive ER stress response. GRP78 is a critical regulator of the unfolded protein response (UPR), which facilitates proper folding of proteins and thus maintains ER functionality, but an excessive ER stress response could lead to cell apoptosis [46, 47]. In this study, BRCA1 knockout enhanced apoptosis induced by ER stress, suggesting that in rapid antler regeneration, BRCA1 may protect the ability of cells to survive by alleviating the ER stress response. In addition, BRCA1 was

(See figure on next page.)

Fig. 6 BRCA1 deletion induced excessive endoplasmic reticulum (ER) stress response. **A** Relative expression levels of BRCA1 mRNA in the different groups after TM treatment; data are shown as the mean ± SEM, n = 3, $^{**}p < 0.01$, $^{****}p < 0.0001$. **B** Western blot analysis of GRP78 protein expression. **C** and **D** Relative expression levels of GRP78 protein (**C**) and mRNA (**D**); note that both protein and mRNA levels in the BRCA1-/- group were higher than in the other groups; data are shown as the mean ± SEM, n = 3, $^{*}p < 0.05$, $^{***}p < 0.001$. **E** Cell apoptosis analysis via flow cytometry after TM-treatment. **F** Percentage of apoptotic cells in the different groups; note that apoptotic cells in the BRCA1-/- group after TM-treatment were significantly higher than those in the other two groups; data are shown as the mean ± SEM, n = 3, $^{*}p < 0.05$, $^{***}p < 0.001$

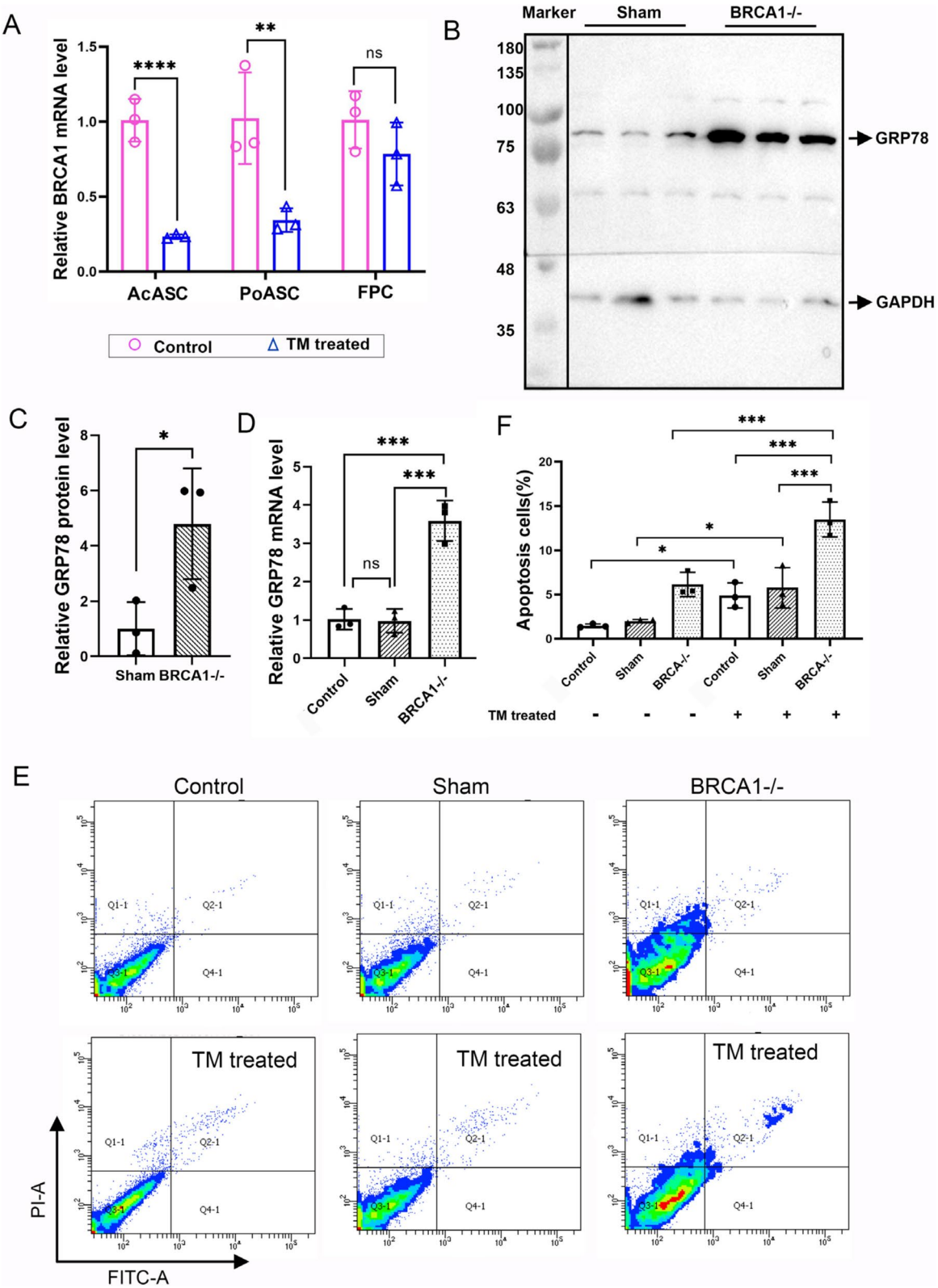

Fig. 6 (See legend on previous page.)

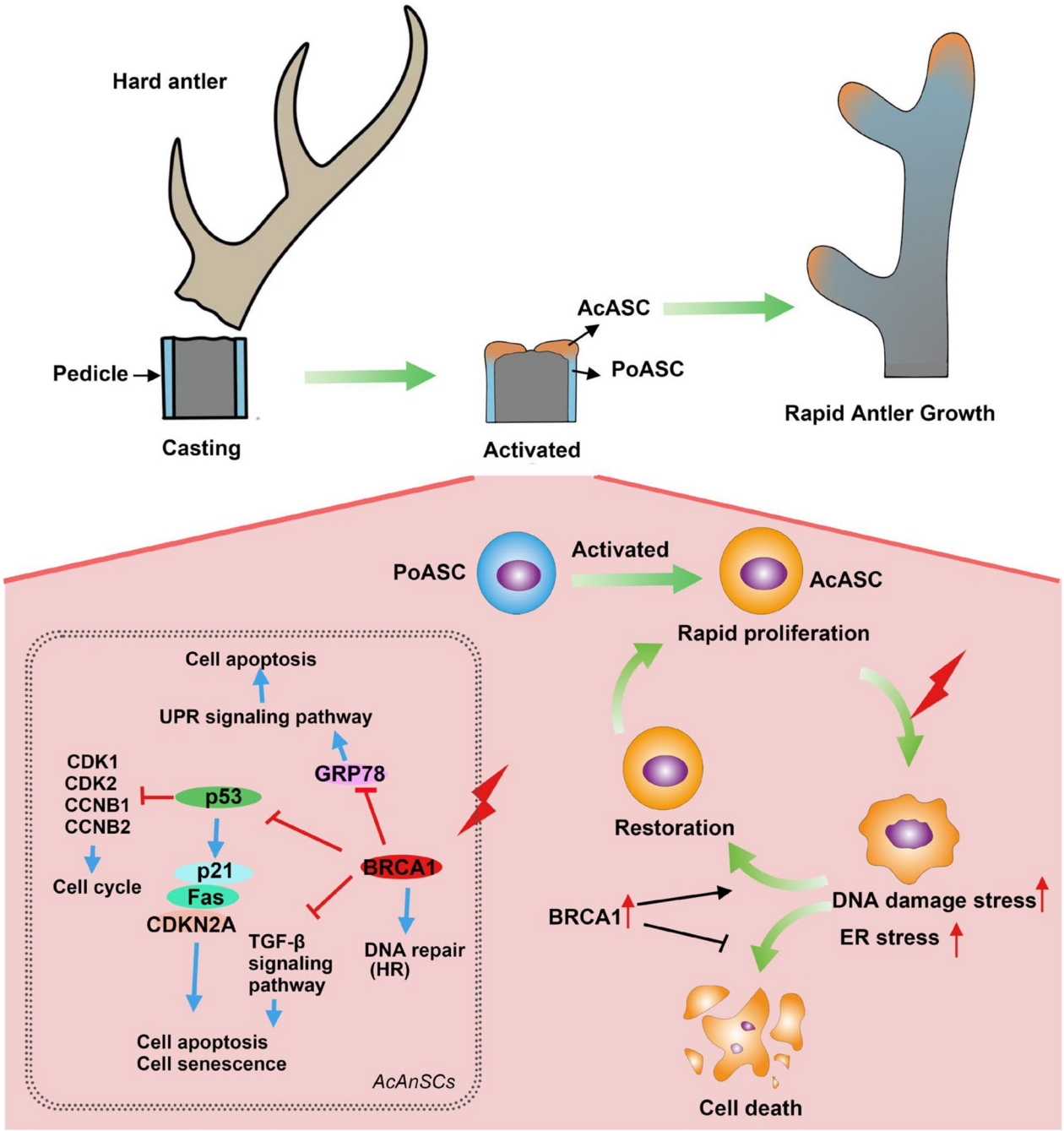

Fig. 7 Hypothetical drawing of the molecular mechanism underlying the roles of BRCA1 in the regulation of rapid antler regeneration and genomic stability. During antler regeneration, rapid cell proliferation tends to cause increased DNA damage stress and ER stress. High expression of BRCA1, on the one hand, may regulate DNA damage response by promoting HR repair, and on the other hand, may inhibit p53/TGF/ER stress-induced cell death, such that cells that have their genomic stability restored continue to enter rapid proliferation mode

recently identified as a novel binding partner of the IP3R1 [48, 49], and BRCA1 over-expression caused an increase in IP3R-mediated Ca^{2+} signaling in HeLa cells [48]. During antler regeneration, the Ca^{2+} signaling pathway is highly activated in the AcAnSCs [13], so the question as to whether the high expression of BRCA1 in the AcAnSCs involves activation of the Ca^{2+} signaling pathway is worthy of further investigation.

Conclusions

In seeking to understand the mechanism underlying the unique phenomenon of very rapid antler regeneration without neoplastic transformation, we screened and identified some key regulators, among which BRCA1 was most prominent. Our results support the hypothesis that BRCA1 is involved in sustaining rapid antler growth via regulation of DNA damage repair, thus effectively helping the maintenance of genomic stability and balancing of p53/ERS signaling pathway to protect cells from apoptosis. We believe that our findings as to how genomic stability is maintained in the rapidly-proliferating cells of the antler during regeneration is of great significance not only for the understanding of regenerative medicine, but also for cancer development.

Supplementary Information

The online version contains supplementary material available at https://doi.org/10.1186/s13062-025-00606-1.

Supplementary Material 1

Supplementary Material 2

Acknowledgements

We would like to thank Dr Peter Fennessy for critically reading through the manuscript and staff from Institute of Antler Science and Product Technology, Changchun Sci-Tech University, for the help of collection of antler stem cells.

Author contributions

QG and CL conceived and designed the experiment. QG, ZW, JL, CM and GZ performed the experiments. JZ and HB performed bioinformatics and statistical analyses. QG, GZ and CL drafted and revised the manuscript. All authors read and approved the final manuscript.

Funding

This work was supported by National Natural Science Foundation of China (Grant Numbers: U23A20523; 32301151), Science and Technology Development Plan Project of Jilin Province (Grant Numbers: YDZJ202201ZYTS435), the Doctoral Research Start-Up Fund of Changchun Sci-Tech University (Grant No. 202304), and the Chinese Key Natural Science Foundation (Regional Joint Funds; U20A20403).

Availability of data and materials

The datasets generated during the current study are available in the NCBI Sequence Read Archive (SRA) under accession number SAMN45127279. The link is https://dataview.ncbi.nlm.nih.gov/object/SAMN45127279.

Declarations

Ethics approval and consent to participate

Not applicable.

Consent for publication

Not applicable.

Competing interests

The authors declare no competing interests.

Author details

[1]Institute of Antler Science and Product Technology, Changchun Sci-Tech University, Changchun, Jilin, China. [2]Institute of Special Animal and Plant Sciences, Chinese Academy of Agricultural Sciences, Changchun, Jilin, China.

Received: 20 December 2024 Accepted: 14 January 2025
Published online: 24 January 2025

References

1. Wang N, Xu S, Egli D. Replication stress in mammalian embryo development, differentiation, and reprogramming. Trends Cell Biol. 2023;33:872–86.
2. Sarig R, Tzahor E. The cancer paradigms of mammalian regeneration: can mammals regenerate as amphibians? Carcinogenesis. 2017;38:359–66.
3. Charni M, Aloni-Grinstein R, Molchadsky A, Rotter V. p53 on the crossroad between regeneration and cancer. Cell Death Differ. 2017;24:8–14.
4. Beachy PA, Karhadkar SS, Berman DM. Tissue repair and stem cell renewal in carcinogenesis. Nature. 2004;432:324–31.
5. Schafer M, Werner S. Cancer as an overhealing wound: an old hypothesis revisited. Nat Rev Mol Cell Biol. 2008;9:628–38.
6. Qin T, Zhang G, Zheng Y, Li S, Yuan Y, Li Q, et al. A population of stem cells with strong regenerative potential discovered in deer antlers. Science. 2023;379:840–7.
7. Li C. Deer antler regeneration: a stem cell-based epimorphic process. Birth Defects Res C Embryo Today. 2012;96:51–62.
8. Li C, Li Y, Wang W, Scimeca M, Melino G, Du R, et al. Deer antlers: the fastest growing tissue with least cancer occurrence. Cell Death Differ. 2023;30(12):2452–61.
9. Wang Y, Zhang C, Wang N, Li Z, Heller R, Liu R, et al. Genetic basis of ruminant headgear and rapid antler regeneration. Science. 2019;364:eaav6335.
10. Goss RJ. Deer antlers: regeneration, function, and evolution. Cambridge: Academic Press; 1983.
11. Li C, Suttie JM, Clark DE. Histological examination of antler regeneration in red deer (Cervus elaphus). Anat Rec. 2005;282A:163–74.
12. Li C, Mackintosh CG, Martin SK, Clark DE. Identification of key tissue type for antler regeneration through pedicle periosteum deletion. Cell Tissue Res. 2007;328:65–75.
13. Guo Q, Zheng J, Ba H, Sun H, Zhai J, Wang W, et al. Calreticulin identified as one of the androgen response genes that trigger full regeneration of the only capable mammalian organ, the deer antler. Front Cell Dev Biol. 2022;10: 862841.
14. Li C, Zhao H, Liu Z, McMahon C. Deer antler—a novel model for studying organ regeneration in mammals. Int J Biochem Cell Biol. 2014;56:111–22.
15. Li C, Suttie JM. Light microscopic studies of pedicle and early first antler development in red deer (Cervus elaphus). Anat Rec. 1994;239:198–215.
16. Wang D, Berg D, Ba H, Sun H, Wang Z, Li C. Deer antler stem cells are a novel type of cells that sustain full regeneration of a mammalian organ-deer antler. Cell Death Dis. 2019;10(6):443.
17. Li C, Chu W. The regenerating antler blastema the derivative of stem cells resident in a pedicle stump. Front Biosci. 2016;21:455–67.
18. El-Andaloussi S, Lee Y, Lakhal-Littleton S, Li J, Seow Y, Gardiner C, et al. Exosome-mediated delivery of siRNA in vitro and in vivo. Nat Protoc. 2012;7:2112–26.
19. Xing X, Ai C, Wang T, Li Y, Liu H, Hu P, et al. The first high-quality reference genome of sika deer provides insights for high-tannin adaptation. Genomics Proteomics Bioinform. 2023;21:203–15.
20. Chin CH, Chen SH, Wu HH, Ho CW, Ko MT, Lin CY. cytoHubba: identifying hub objects and sub-networks from complex interactome. BMC Syst Biol. 2014;8:S11.
21. Tang Y, Li M, Wang J, Pan Y, Wu FX. CytoNCA: a cytoscape plugin for centrality analysis and evaluation of protein interaction networks. Biosystems. 2015;127:67–72.
22. Tarsounas M, Sung P. The antitumorigenic roles of BRCA1-BARD1 in DNA repair and replication. Nat Rev Mol Cell Biol. 2020;21:284–99.
23. Hromas R, Srinivasan G, Yang M, Jaiswal A, Totterdale TA, Phillips L, et al. BRCA1 mediates protein homeostasis through the ubiquitination of PERK and IRE1. iScience. 2022;25:105626.
24. Rawashdeh RR, Pederson H, Iskanderian R, Khan F, Altrabulsi B, et al. Germline mutations of the BRCA1 gene in breast, ovarian cancer families: evidence for a genotype/phenotype correlation. Nat Genet. 1995;11:428–33.
25. Tarsounas M, Sung P. The antitumorigenic roles of BRCA1–BARD1 in DNA repair and replication. Nat Rev Mol Cell Biol. 2020;21:284–99.

26. Shakya R, Szabolcs M, McCarthy E, Ospina E, Basso K, Nandula S, et al. The basal-like mammary carcinomas induced by Brca1 or Bard1 inactivation implicate the BRCA1/BARD1 heterodimer in tumor suppression. Proc Natl Acad Sci USA. 2008;105:7040–5.
27. Li X, Zou L. BRCAness, DNA gaps, and gain and loss of PARP inhibitor-induced synthetic lethality. J Clin Invest. 2024. https://doi.org/10.1172/JCI181062.
28. Werner H. BRCA1: an endocrine and metabolic regulator. Front Endocrinol (Lausanne). 2022;13: 844575.
29. Hakem R, de la Pompa JL, Sirard C, Mo R, Woo M, Hakem A. The tumor suppressor gene Brca1 is required for embryonic cellular proliferation in the mouse. Cell. 1996;85:1009–23.
30. Satterwhite DJ, Matsunami N, White RL. TGF-b1 inhibits BRCA1 expression through a pathway that requires pRb1. Biochem Biophys Res Commun. 2000;276:686–92.
31. Jackson SP, Bartek J. The DNA-damage response in human biology and disease. Nature. 2009;461(7267):1071.
32. Yoshida K, Miki Y. Role of BRCA1 and BRCA2 as regulators of DNA repair, transcription, and cell cycle in response to DNA damage. Cancer Sci. 2004;95(11):866.
33. Paull TT, Cortez D, Bowers B, Elledge SJ, Gellert M. Direct DNA binding by Brca1. Proc Natl Acad Sci USA. 2001;98:6086–91.
34. Daley JM, Niu H, Miller S, Sung P. Biochemical mechanism of DSB end resection and its regulation. DNA Repair. 2015;32:66–74.
35. Bouwman P, Aly A, Escandell JM, Pieterse M, Bartkova J, van der Gulden H, et al. 53BP1 loss rescues BRCA1 deficiency and is associated with triple-negative and BRCA-mutated breast cancers. Nat Struct Mol Biol. 2010;17:688–95.
36. Dai L, Dai Y, Han J, Huang Y, Wang L, Huang J, et al. Structural insight into BRCA1-BARD1 complex recruitment to damaged chromatin. Mol Cell. 2021;81(13):2765-2777.e6.
37. Bunting SF, Callén E, Wong N, Chen HT, Polato F, et al. Gunn A.53BP1 inhibits homologous recombination in brca1-deficient cells by blocking resection of DNA breaks. Cell. 2010;141:243–54.
38. Cejka P, Symington LS. DNA end resection: mechanism and control. Annu Rev Genet. 2021;23:55.
39. Hakem R, de la Pompa JL, Sirard C, Mo R, Woo M, et al. The tumor suppressor gene Brca1 is required for embryonic cellular proliferation in the mouse. Cell. 1996;85:1009–23.
40. Cao L, Kim S, Xiao C, Wang RH, Coumoul X, Wang X, et al. ATM-Chk2-p53 activation prevents tumorigenesis at an expense of organ homeostasis upon Brca1 deficiency. EMBO J. 2006;25:2167–77.
41. Dubrovska A, Kanamoto T, Lomnytska M, Heldin CH, Volodko N, Souchelnytskyi S. (2005) TGFbeta1/Smad3 counteracts BRCA1-dependent repair of DNA damage. Oncogene. 2005;24:2289–97.
42. Li H, Sekine M, Seng S, Avraham S, Avraham HK. BRCA1 interacts with Smad3 and regulates Smad3-mediated TGF-b signaling during oxidative stress responses. PLoS ONE. 2009;4: e7091.
43. Coene E, Van Oostveldt P, Willems K, van Emmelo J, De Potter CR. BRCA1 is localized in cytoplasmic tube-like invaginations in the nucleus. Nat Genet. 1997;16:122–4.
44. De Potter CR, Coene ED, Schelfhout VR. Localization of BRCA1 protein at the cellular level. J Mammary Gland Biol Neoplasia. 1998;3:423–9.
45. Yeung BH, Kwan BW, He QY, Lee AS, Liu J, Wong AS. Glucose-regulated protein 78 as a novel effector of BRCA1 for inhibiting stress-induced apoptosis. Oncogene. 2008;27:6782–9.
46. Guo W, Wang M, Yang Z, Liu D, Ma B, Zhao Y, et al. Recent advances in small molecule and peptide inhibitors of glucose-regulated protein 78 for cancer therapy. Eur J Med Chem. 2023;261: 115792.
47. Zhang W, Shi Y, Oyang L, Cui S, Li S, Li J, et al. Endoplasmic reticulum stress-a key guardian in cancer. Cell Death Discov. 2024;10:343.
48. Hedgepeth SC, Garcia MI, Wagner LE, Rodriguez AM, Chintapalli SV, Snyder RR, et al. The BRCA1 tumor suppressor binds to inositol 1,4,5-trisphosphate receptors to stimulate apoptotic calcium release. J Biol Chem. 2015;290:7304–13.
49. Bittremieux M, Parys JB, Pinton P, Bultynck G. ER functions of oncogenes and tumor suppressors: modulators of intracellular Ca2+ signaling. Biochim Biophys Acta. 2016;1863:1364–78.

Publisher's Note